

Mutational Analysis of the Kinetics and Thermodynamics of Transcription Factor NF- κ B Homodimerisation

Y. S. N. Day,^[a, b] S. L. Bacon,^[b] Z. Hughes-Thomas,^[b] J. M. Blackburn,^[c] and J. D. Sutherland^{*[a, b]}

Dimeric transcription factors of the NF- κ B/Rel family are sequence-specific DNA-binding proteins that mediate the inducible expression of immunologically important eukaryotic genes by competing for κ B sites. The kinetic and thermodynamic components of these interactions were probed by mutation of the subunit interface of the p50 homodimer, a paradigm for other family members. Guided by the crystal structure, we selected the side chains of five key residues (R255, Y270, L272, A311 and V313) for individual and combinatorial truncation, with the aim of generating a mutant panel. Homodimerisation was assessed indirectly by measurement of DNA binding with an optical biosensor in order to unmask the relative contributions of each residue. Surface plasmon resonance revealed that a unanimous bias for a palindromic κ B site over an asymmetric one was mainly the result of a slower dissociation rate for the DNA/homodimer complex in the case of the palindromic κ B

site. Y270 and L272 were individually the most critical residues in homodimerisation. DNA binding was abolished when all five residues were substituted, which reinforces the notion that only a subset of residues contributes crucial dimer-forming contacts. The role of Y270 was unique, since its mutation to glycine dramatically slowed both the association and dissociation rates for DNA binding. Surprisingly, R255 was shown to be of little importance in the stability of the p50 homodimer, despite its apparent participation in a salt bridge at the dimer interface. Our results suggest that binding modes inferred from structural data should be treated cautiously.

KEYWORDS:

DNA recognition • mutagenesis • noncovalent interactions • protein engineering • surface plasmon resonance

Introduction

NF- κ B was first identified as a dimeric nuclear factor that binds the immunoglobulin (Ig) κ light-chain transcriptional enhancer and was apparently active constitutively only in B lymphocytes.^[1] These factors are comprised of p50 and p65 subunits, both of which exhibit homology to the cRel proto-oncogene product. Numerous transcription factors have since been characterised that share the Rel homology region (RHR) in their N-terminal region, which defines both their dimerisation and DNA-binding properties. These transcription factors appear to be ubiquitously expressed in all mammalian cells.^[2] In the resting state, dimeric NF- κ B is cytoplasmically retained through the masking of its C-terminal nuclear localisation signals (NLSs) by a monomeric regulatory protein, I- κ B.^[3] The activation of NF- κ B factors is post-translationally induced in response to diverse signals that trigger the phosphorylation and proteolytic degradation of I- κ B by a ubiquitin-mediated cascade pathway. The consequently unmasked NLSs of NF- κ B cause it to be targeted for rapid transport to the nucleus, where it competes with other NF- κ B dimers for binding to specific DNA sequences, termed κ B motifs. Target sites are present in the enhancers of a variety of immunologically important eukaryotic genes, which include those involved in cellular growth, development, carcinogenesis and the proliferation of viruses, for example, the human immunodeficiency virus.^[4] Combinatorial pairing of NF- κ B subunits (p50, p52, p65,


RelB and cRel) increases the repertoire of κ B motifs for which the NF- κ B dimers compete and modulates the inducible transcription and hence expression of a variety of target genes.

The strikingly butterfly-like crystal structure of homodimeric p50 bound to a κ B site, published simultaneously by two groups, formed the foundation for our work as it is representative of the RHR shared by other members of the NF- κ B/Rel family of transcription factors.^[5] Each subunit folds into two distinct Ig-like domains that are tethered by a flexible hinge segment. Sequence-specific DNA binding is mediated through residues in well-defined loops, which are contributed by both domains

[a] Prof. J. D. Sutherland, Y. S. N. Day
Department of Chemistry
The University of Manchester, Oxford Road
Manchester M13 9PL (UK)
Fax: (+44) 161-275-4939
E-mail: john.sutherland@man.ac.uk

[b] Prof. J. D. Sutherland, Y. S. N. Day, S. L. Bacon, Z. Hughes-Thomas
The Dyson Perrins Laboratory
University of Oxford (UK)

[c] Dr. J. M. Blackburn
Department of Biochemistry
University of Cambridge (UK)

 Supporting information for this article is available on the WWW under <http://www.chembiochem.org> or from the author.

and together form a continuous DNA–protein interface. In contrast, dimerisation contacts emanate solely from the C-terminal domain, the core of which is formed by a set of interdigitating hydrophobic residues and is flanked by a network of polar contacts (Figure 1). These residues are highly conserved within the NF- κ B/Rel family.

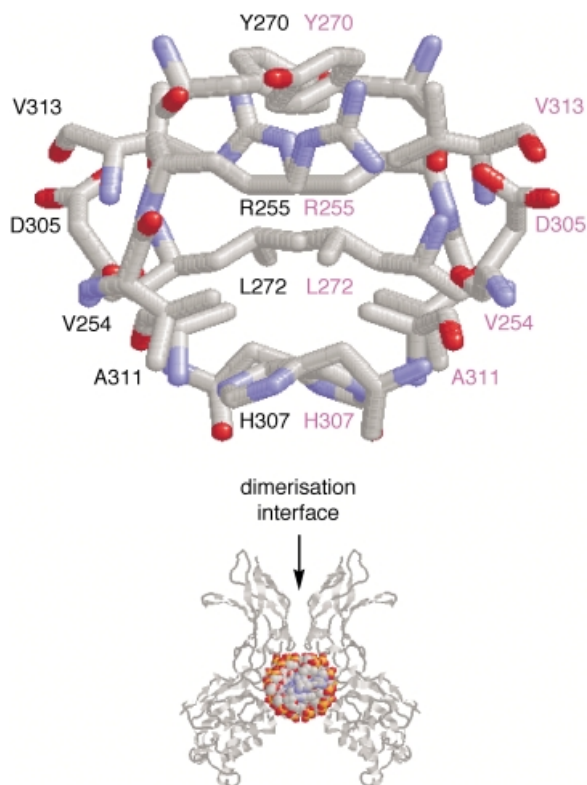


Figure 1. Core residues that form dimer interface contacts in the p50 homodimer viewed along the DNA axis with the dyad vertical. Residues contributed by each monomer are distinguished by label colour (black or pink).

Recent studies on the effect of alanine substitutions at ten p50 homodimer-forming residues by a combination of chemical cross-linking, size-exclusion chromatography and sedimentation equilibrium methods suggested a “hot spot” of intersubunit interactions.^[6] Residue Y270 was implicated as the most important for stabilisation of the dimer interface. We employed a truncated construct of p50 that retained only wild-type dimerisation functions. We have previously investigated dimerisation by using a linked reporter gene diversity screening approach for which a library of mutants was constructed.^[7] Simultaneous randomisation of four residues at the dimer interface (Y270, L272, A311 and V313) allowed selection of twentyfive novel functional interfaces that repressed the reporter gene to levels similar to that achieved by the wild-type protein. The L272/A311 core was repeatedly, but not always, selected from the library, while a range of predominantly nonpolar residues were selected at positions 270 and 313. These results indicate that L272 and A311 form a hot spot of interaction.

The roles of five homodimer-forming residues in DNA binding are investigated in this paper. The side chains of five key amino acids, R255, Y270, L272, A311 and V313, located at the dimer interface with no direct contact with DNA, were candidates for mutational truncation. The effect of these substitutions on p50 homodimerisation was evaluated indirectly by measuring the DNA-binding properties of the p50 variants affected at the dimer interface. By unmasking the kinetic profiles of these variants, we shed new light on the mechanism of the sequence-specific DNA binding events of these biologically important dimers.

Results and Discussion

Use of a recombinant analogue of NF- κ B p50 to facilitate cassette mutagenesis

A truncated and recombinant analogue of human wild-type NF- κ B p50 (p50RHR) that encodes a minimal RHR (residues 40–366) was designed for the generation of mutants by a cassette-based strategy. This analogue was derived from vector pLM1-p50, which retained wild-type activity for homodimerisation, DNA binding and interaction with its regulatory partner, protein I κ B.^[5] Our semisynthetic construct introduced three conservative mutations (Y286F, G297A and K318A) and additional cloning sites (see the Supporting Information). We envisaged an extensive series of mutants and therefore constructed a vector (pTFM4) that expresses a fusion protein that could be purified rapidly in a single elution step with maltose-containing buffers and an amylose-based affinity column. Maltose-binding protein (MBP) was a suitable fusion partner since wild-type p50 tolerates fusions at either terminus with no apparent loss of DNA binding affinity (unpublished results). This is consistent with termini remote from the functional domains, surface-exposed and disordered, as shown by crystallographic data.^[5] A total of 19 dimer interface mutants (Figure 2) were created by a series of cassette replacements and expressed as MBP fusions (see the Supporting Information). To assess the validity of our recombinant analogue, comparison was made with an MBP-fused version of the pLM1-p50-derived wild-type p50 prepared from cells transformed with pRES101.^[8]

Surface plasmon resonance (SPR) as a biophysical tool

κ B site-dependent binding was investigated by using two different targets (see the Experimental Section). One sequence was a previously uncharacterised idealised palindrome (5'-gggaattccc-3') derived from the major histocompatibility complex class I gene enhancer. The other was a physiologically relevant asymmetric consensus sequence (5'-GGGACTTCC-3') preferred by the p50/p65 heterodimer, the prototypic and most naturally prevalent dimer in the NF- κ B family. A Biacore 3000 surface plasmon resonance optical biosensor equipped with a streptavidin-coated sensor chip was used to monitor the association and dissociation rates of DNA/protein complexes in real time. Double-stranded DNA probes carrying the target κ B sites were captured onto the sensor surface through a biotin moiety on one strand. A probe in which the κ B site was replaced

250	260	270	280	290	300	310	MBP-fused protein
NLKIVRMDRT	AGCVTGGEEI	YLL CDKVQKD	DIQIRFEEEE	ENGGVWEaFG	DFSPTDVHRQ	FAIV FKTPKY	Wild-type
NLKIVRMDRT	AGCVTGGEEI	YLL CDKVQKD	DIQIRFEEEE	ENGGVWEaFG	DFSPTDVHRQ	FAIV FKTPaY	p50RHR
NLKIVRMDRT	AGCVTGGEEI	YLL CDKVQKD	DIQIRFEEEE	ENGGVWEaFG	DFSPTDVHRQ	FAIV FKTPaY	p50 (R255A)
NLKIVRMDRT	AGCVTGGEEI	GLL CDKVQKD	DIQIRFEEEE	ENGGVWEaFG	DFSPTDVHRQ	FAIV FKTPaY	p50 (Y270G)
NLKIVRMDRT	AGCVTGGEEI	YLL CDKVQKD	DIQIRFEEEE	ENGGVWEaFG	DFSPTDVHRQ	FAIV FKTPaY	p50 (L272I)
NLKIVRMDRT	AGCVTGGEEI	YLL CDKVQKD	DIQIRFEEEE	ENGGVWEaFG	DFSPTDVHRQ	FAIV FKTPaY	p50 (L272A)
NLKIVRMDRT	AGCVTGGEEI	YLG CDKVQKD	DIQIRFEEEE	ENGGVWEaFG	DFSPTDVHRQ	FAIV FKTPaY	p50 (L272G)
NLKIVRMDRT	AGCVTGGEEI	YLL CDKVQKD	DIQIRFEEEE	ENGGVWEaFG	DFSPTDVHRQ	FGIA FKTPaY	p50 (A311G)
NLKIVRMDRT	AGCVTGGEEI	YLL CDKVQKD	DIQIRFEEEE	ENGGVWEaFG	DFSPTDVHRQ	FAIA FKTPaY	p50 (V313A)
NLKIVRMDRT	AGCVTGGEEI	YLL CDKVQKD	DIQIRFEEEE	ENGGVWEaFG	DFSPTDVHRQ	FAIV FKTPaY	p50 (R255A, Y270G)
NLKIVRMDRT	AGCVTGGEEI	YLL CDKVQKD	DIQIRFEEEE	ENGGVWEaFG	DFSPTDVHRQ	FAIV FKTPaY	p50 (R255A, L272I)
NLKIVRMDRT	AGCVTGGEEI	YLL CDKVQKD	DIQIRFEEEE	ENGGVWEaFG	DFSPTDVHRQ	FAIV FKTPaY	p50 (R255A, L272A)
NLKIVRMDRT	AGCVTGGEEI	YLG CDKVQKD	DIQIRFEEEE	ENGGVWEaFG	DFSPTDVHRQ	FAIV FKTPaY	p50 (R255A, L272G)
NLKIVRMDRT	AGCVTGGEEI	YLL CDKVQKD	DIQIRFEEEE	ENGGVWEaFG	DFSPTDVHRQ	FGIV FKTPaY	p50 (R255A, A311G)
NLKIVRMDRT	AGCVTGGEEI	YLL CDKVQKD	DIQIRFEEEE	ENGGVWEaFG	DFSPTDVHRQ	FAIA FKTPaY	p50 (R255A, V313A)
NLKIVRMDRT	AGCVTGGEEI	GLG CDKVQKD	DIQIRFEEEE	ENGGVWEaFG	DFSPTDVHRQ	FAIV FKTPaY	p50 (Y270G, L272G)
NLKIVRMDRT	AGCVTGGEEI	YLL CDKVQKD	DIQIRFEEEE	ENGGVWEaFG	DFSPTDVHRQ	FGIA FKTPaY	p50 (A311G, V313A)
NLKIVRMDRT	AGCVTGGEEI	GLG CDKVQKD	DIQIRFEEEE	ENGGVWEaFG	DFSPTDVHRQ	FAIV FKTPaY	p50 (R255A, Y270G, L272G)
NLKIVRMDRT	AGCVTGGEEI	YLL CDKVQKD	DIQIRFEEEE	ENGGVWEaFG	DFSPTDVHRQ	FGIA FKTPaY	p50 (R255A, Y270G, A311G, V313A)
NLKIVRMDRT	AGCVTGGEEI	YLG CDKVQKD	DIQIRFEEEE	ENGGVWEaFG	DFSPTDVHRQ	FGIA FKTPaY	p50 (R255A, L272G, A311G, V313A)
NLKIVRMDRT	AGCVTGGEEI	GLG CDKVQKD	DIQIRFEEEE	ENGGVWEaFG	DFSPTDVHRQ	FGIA FKTPaY	p50 (R255A, Y270G, L272G, A311G, V313A)

Figure 2. Partial amino acid sequence alignment (residues 250–319) of recombinant wild-type human NF- κ B p50, our recombinant analogue (p50RHR) and nineteen derivatives. The five key dimer interface residues selected for mutational truncation are boxed in yellow. Substitutions are denoted in red. The three conservative mutations (Y286F, G297A and K318A) imposed in the design of our minimal construct are denoted in lower case. The corresponding wild-type residues are indicated in bold. The numbering follows that reported for the crystal structure of the p50 homodimer clamping DNA elucidated by Muller et al.^[5]

by an irrelevant 10-bp sequence served as a control. Protein injections were analysed simultaneously across differently derivatised flow cells. One flow cell was left unmodified to provide a reference surface.

Although replicate DNA binding responses were highly reproducible across freshly captured probes, the surface decayed over time. This was attributed to the gradual dissociation of the duplex probes as a single strand separated from its complement bound onto pre-immobilized streptavidin. Proteins were analysed at three concentrations in a high-throughput screen across newly captured probes to ensure a stable surface during the assay. Global analysis unmasked the kinetics of these sequence-specific binding events.

Use of a dense surface

Near-equilibrium binding was attempted at a 5- μ L min⁻¹ flow rate across densely captured probes (~100 RU). The affinity of recombinant p50RHR for the natural asymmetric κ B site was determined by conduction of a high-resolution-mode analysis in a buffer that contained 100 mM NaCl by injection of protein at a wide range of concentrations (the maximum concentration was 2000 times the minimum value). Homodimer bound the target specifically, in a concentration-dependent manner and saturated all binding sites above a critical protein concentration. The observed surface capacity was consistent with that expected for the molecular weight of homodimeric MBP-p50RHR (158 kDa) binding DNA in a 1:1 stoichiometry. It was also consistent with two monomers binding their κ B-half-site targets. Despite a prolonged association phase, not all binding responses attained equilibrium, which is characteristic of the high affinity DNA binding mode of transcription factors.^[9] Therefore, the data could not be described by an equilibrium binding isotherm. The affinity was instead estimated by a kinetic interpretation of the binding data. The kinetics of DNA binding for the p50RHR

homodimer were too complex to be described accurately by any available model in the software, however, a reasonable simulation was returned by global analysis with a mass transport model that estimated the affinity to be 3 nM (Figure 3). Collection of binding data across a densely captured probe at a very slow flow rate led to masking of the true DNA binding kinetics since it imposed further mass transport limitations on an already transport-influenced interaction. This problem was suggested by the strong flow-rate dependence of binding curves (data not shown) and was also observed by Hart et al.^[10] The effect of single alanine substitutions at positions R255 and L272 were assessed without any further data fitting. Surprisingly, given the apparent participation of R255 in a salt bridge at the dimer interface, R255A homodimers appeared only marginally defective in DNA binding. In contrast, L272A homodimers were markedly more defective, mainly as a result of a more rapid dissociation rate than for the R255A homodimers, which suggested that residue L272 is more critical in p50 homodimerisation than R255.

Recent solution-based equilibrium studies by Phelps et al.^[11] on wild-type p50 homodimer binding to an asymmetric κ B site agreed with our surface-based near-equilibrium measurements in two respects. First, the equilibrium studies tested only the RHR portion of p50 and reported its DNA binding affinity to be in the low nanomolar range: affinity, $K_D = 54.3 \pm 1.1$ nM (fluorescence anisotropy method at pH 7.5) and 85.3 ± 0.6 nM (electrophoretic mobility shift assay at pH 8.0). Secondly, the binding data reported by Phelps et al. deviated from a simple model and fit best to a cooperative one that describes two monomers assembling sequentially on DNA. The use of a shorter duplex probe and a different buffer system in the studies by Phelps et al. compared to our near-equilibrium experiments may have contributed to the discrepancy between the estimated affinities, since Phelps et al. observed a strong pH and salt dependence for DNA binding.

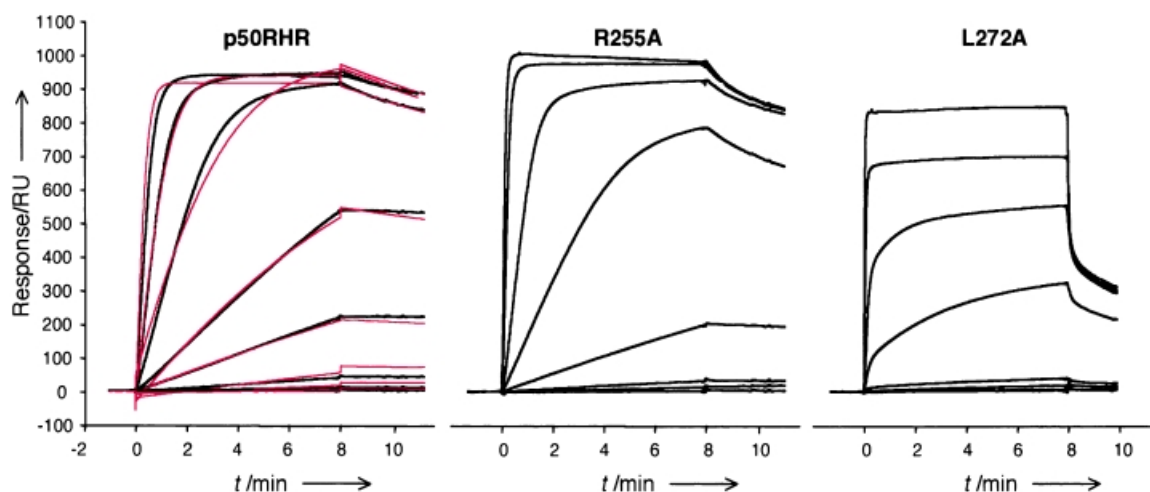


Figure 3. Comparative analysis of 0.46–1000 nM p50RHR homodimer and two single alanine mutants binding an asymmetric κ B site. Proteins were diluted in buffer that contained 100 mM NaCl and injected at $5 \mu\text{L min}^{-1}$ across a densely captured probe. Global analysis (red lines) of binding responses (black lines) with a mass transport model returned an affinity of 2.70 ± 0.07 nM from the reaction rate constants of $k_a = (1.2 \pm 0.2) \times 10^5 \text{ M}^{-1} \text{ s}^{-1}$ and $k_d = (3.21 \pm 0.09) \times 10^{-4} \text{ s}^{-1}$. Under these experimental conditions (not ideal for kinetic interpretation) the diffusion-limited rate constant $k_m = (5.86 \pm 0.08) \times 10^7 \text{ RU M}^{-1} \text{ s}^{-1}$ varied by two orders of magnitude from the predicted value for a 158-kDa analyte of $1.2 \times 10^9 \text{ RU M}^{-1} \text{ s}^{-1}$. For details of the model and definitions of constants, see the Experimental Section.

Use of a low density surface

Switching to a higher flow rate and a lower density of the captured probe removed many artefacts that had obscured the DNA binding reaction of p50 homodimers analysed under near-equilibrium conditions. However, reaction kinetics still deviated from a simple model, likely because of an inherently complex mechanism that could not be dissected by SPR. To a first approximation however, reasonable simulations were returned by using a mass transport model, which extended the range of association rates and thus affinities that could be determined.^[12]

The DNA binding mechanism of p50 probably involves multiple pathways. The assembly state of wild-type p50, analysed at low micromolar concentrations by Sengchanthlangsy et al. in solution-based sedimentation studies,^[6] was best described by a monomer:dimer:tetramer model. This result suggests that all three species are candidates for DNA recognition. At the nanomolar concentrations used in our analysis, it is unlikely that p50 was fully dimeric. If dimerisation occurred upon DNA binding, a cooperative mechanism could be invoked in which monomers bind adjacent half-sites sequentially.^[11] Since the dimerisation domain of the p50 homodimer is not altered by DNA binding,^[13] major structural reorganisation of this domain on DNA is unlikely, although a conformational change may occur in the other domain. The mass transport model used in this study to describe biosensor data grossly over-simplified the reaction mechanism by assuming that a preformed dimer in solution binds DNA in a single step following its diffusion- and flow-limited transport to the captured target on the sensor surface. However, simulations with the biosensor data returned reasonable rate constants and sufficed to compare the DNA binding profiles of the mutant panel.

SPR revealed dramatic kinetic differences in the DNA binding of p50 variants

During validation of the role of our p50RHR species as a wild-type analogue from which all mutants were derived, binding was investigated by SPR in a physiologically relevant buffer that contained 150 mM NaCl and was conveniently supplied by the manufacturer. Wild-type p50 (pRES101), p50RHR (pTFM4) and three p50 mutant proteins were screened for binding to an asymmetric κ B site (Figure 4A). SPR demonstrated that the binding responses generated for wild-type p50 and recombinant p50RHR were virtually identical, which confirms that the reaction kinetics were not affected by our three conservative mutations. Global analysis with a mass transport model yielded affinity constant estimates of 0.650 ± 0.005 and 0.70 ± 0.02 nM for the wild type and mutant species, respectively (Figure 4B). The two proteins also showed indistinguishable binding profiles for the palindromic sequence (data not shown).

Inspection alone shows that SPR revealed dramatic differences in the DNA binding profiles of our panel of p50 mutants binding to an asymmetric κ B site. In corroboration with our studies on a dense surface, a marginally altered affinity was obtained for p50(R255A) homodimers ($K_D = 2.05 \pm 0.03$ nM) compared to the wild type. This result conflicted with the apparently crucial role of R255 in homodimerisation derived from crystallographic data.^[5] When R255A was combined with L272G as a double mutation, homodimerisation/DNA binding was severely affected, as evidenced by the 300-fold weaker DNA binding affinity ($K_D = 240 \pm 30$ nM) of the mutant compared with wild-type p50. The multiple mutant p50(R255A,L272G,A311G,V313A) showed an even weaker DNA binding affinity ($K_D = 520 \pm 70$ nM), comparable to the square-shaped curves that characterised non-specific interactions with the irrelevant probe (blue lines in Figure 4A). These low-affinity interactions ($\approx 0.3 \mu\text{M}$) likely re-

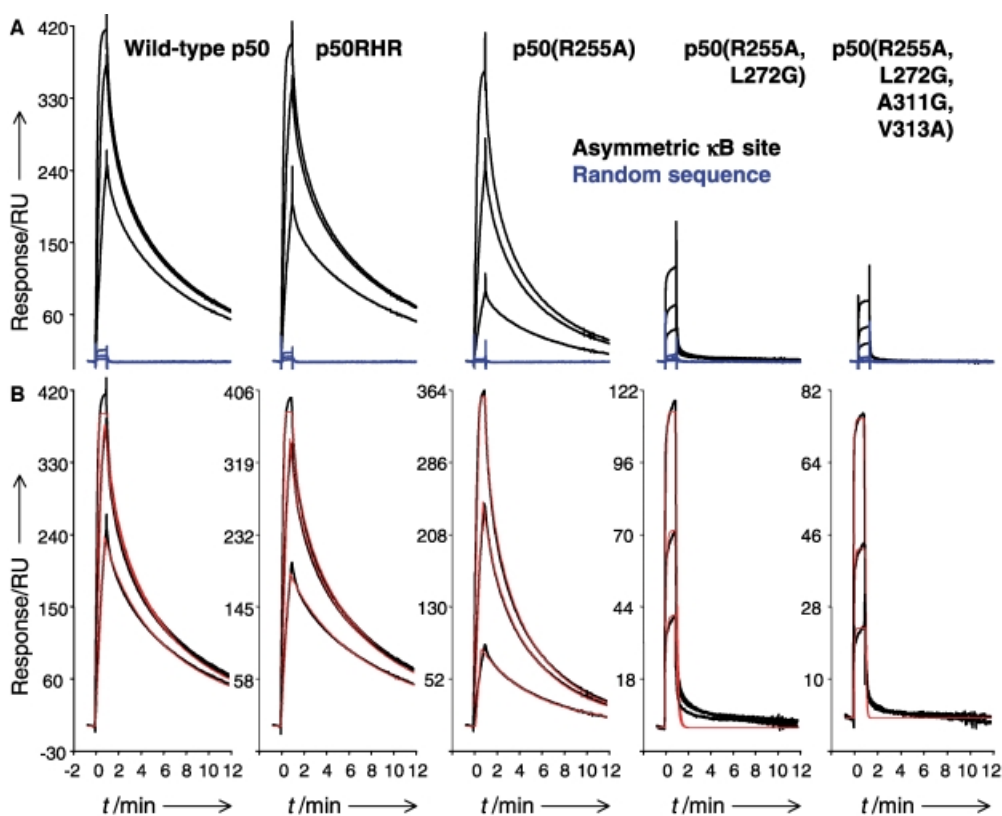


Figure 4. SPR revealed dramatic differences in the DNA binding kinetics of p50 homodimers. A) Binding responses to an asymmetric κ B site (black curves) and a negative control sequence (blue curves). Curves are represented on the same scale to emphasise their differences. Samples were diluted in HBS-P running buffer that contained 150 mM NaCl, and injected at $40 \mu\text{L min}^{-1}$ across probes captured at approximately 40 RU. Wild-type, p50RHR and p50(R255A) homodimers were screened at 5, 10 and 20 nM, whereas the multiple variants were screened at 40, 80 and 160 nM (assuming dimers present). After each interaction cycle, the sensor surface was regenerated with a single 15-s pulse of 0.07% SDS. B) Global analysis of binding responses (black lines) with a mass transport model (red lines). Maximal responses were approximately normalised for clarity. DNA binding affinities were estimated to be: wild-type, $0.650 \pm 0.005 \text{ nM}$; p50RHR, $0.70 \pm 0.02 \text{ nM}$; p50(R255A), $2.05 \pm 0.03 \text{ nM}$; p50(R255A,L272G), $240 \pm 30 \text{ nM}$; p50(R255A,L272G,A311G,V313A), $520 \pm 70 \text{ nM}$. The mean average k_m estimate for the five proteins was $(6 \pm 4) \times 10^9 \text{ RU M}^{-1} \text{ s}^{-1}$, which was close to the predicted value for a 158-kDa analyte of $2 \times 10^9 \text{ RU M}^{-1} \text{ s}^{-1}$.

flected random sampling of DNA sequences in the quest for a κ B site.

Discrimination for a palindromic κ B site

The preference of p50 homodimers for perfectly palindromic κ B sites over asymmetric ones is known,^[14] but here we report a direct comparison of binding to both sequences in real-time in order to unmask the kinetic differences. Studies were conducted at 100 mM NaCl at low capture levels of both probes. A survey of a panel of combinatorialised p50 homodimer variants (Figure 5) demonstrated a unanimous bias for the palindrome, which our analysis attributed mainly to a slower dissociation rate of the DNA/protein complex with the palindromic site. The recombinant wild-type p50 analogue (p50RHR) bound the palindromic κ B site with a 14-fold higher affinity than that observed for the asymmetric one ($K_D = 7$ and $100 \mu\text{M}$, respectively). High affinities for palindromic or pseudopalindromic κ B sites characterise homodimers of the NF- κ B family, as demonstrated by Duckett et al., who estimated the K_D values to be 69.1 and $3.9 \mu\text{M}$ for p49 and p50 homodimers, respectively, binding the HIV κ B site (5'-

GGGGATCCCC-3').^[14] Picomolar DNA binding affinities were measured for all p50 homodimer variants tested with the palindromic κ B site, which approached the detection limit of the biosensor. In contrast, the asymmetric κ B site was bound with affinities that ranged from low picomolar to high nanomolar values.

Effect of amino acid substitutions on p50 homodimerisation

Deviations from wild-type NF- κ B p50 DNA binding reflected the different roles played by the five selected residues in homodimerisation (Figure 5). p50(R255A) and p50(L272I) variants retained picomolar affinities for both sequences, which demonstrates that these single mutations did not significantly modulate the dimer interface.

The diverse stabilities of the protein/DNA complexes with both κ B sites were found to result from an interplay of association and dissociation rates, with more variation in dissociation. The mutant

p50(Y270G) displayed a distinctly lower association rate than wild-type p50, but also a low dissociation rate. This implies that loss of the natural phenolic side chain slows the homodimerisation or DNA recognition step but once assembled on DNA, the complex is stable. Y270 thus appears the most critical individual residue in homodimerisation/DNA binding, since the glycine substitution dramatically lowers the DNA binding affinity of the resultant homodimers. Of the five residues selected in this study, Y270 was the only nonidentical conserved residue within the Rel/NF κ B family. In p65 the corresponding residue is a phenylalanine, which presumably impairs homodimerisation as a result of loss of hydrogen bond contacts. One may speculate that this substitution contributes to the low natural abundance of the p65 homodimer.

Surprisingly, a single alanine substitution at position R255 resulted in homodimers with apparently unaltered wild-type DNA binding affinity. This observation agreed with solution-based sedimentation equilibrium measurements of p50dd variants made by Sengchanthalangsy et al.^[6]

The exchange of leucine at position 272 for its isomer isoleucine had only a minimal effect, yet truncation to the smaller side chains of alanine or glycine dramatically impaired

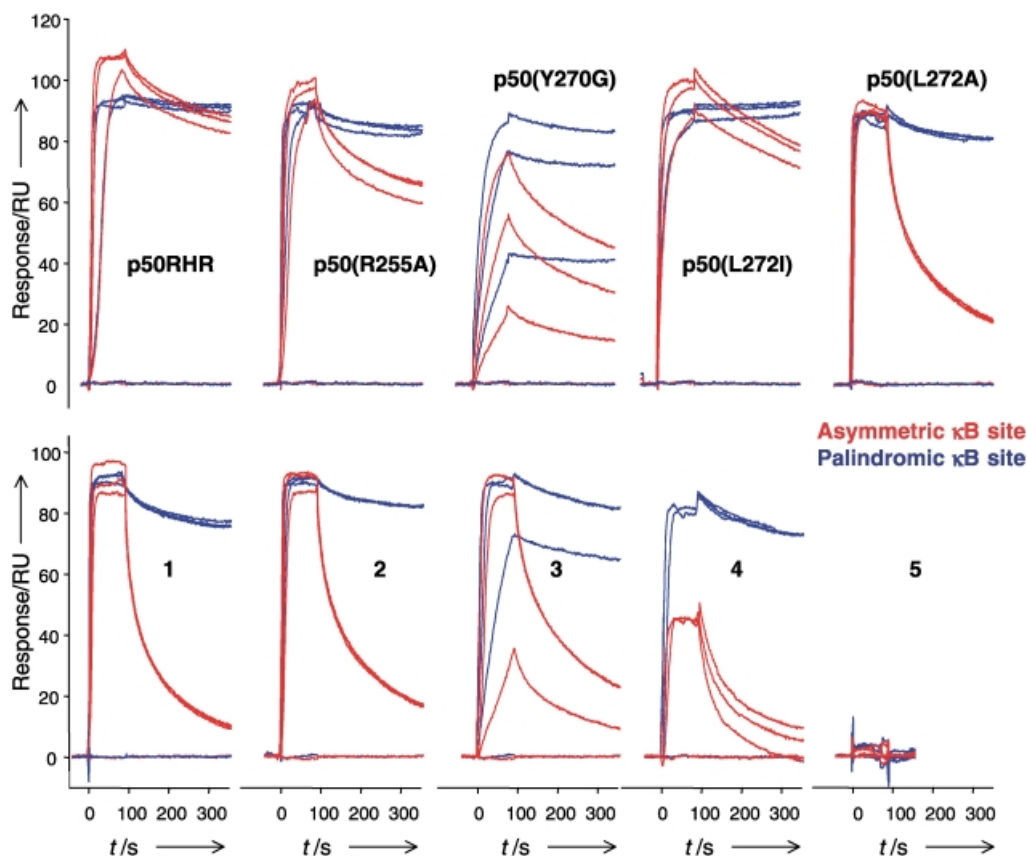


Figure 5. Interaction analysis for a panel of selected p50 mutants revealed a unanimous bias in favour of a palindromic κ B site (blue) over an asymmetric one (red). Binding responses were highly reproducible (data not shown). Single mutants were screened at 0, 20, 40 and 80 nM (upper panel) and multiple mutants (numbered 1–5) were analysed at 0, 40, 80 and 160 nM (lower panel): 1 = p50(R255A,L272A), 2 = p50(Y270G,L272G), 3 = p50(A311G,V313A), 4 = p50(R255A,Y270G,A311G,V313A) and 5 = p50(R255A,Y270G,L272G,A311G,V313A). Samples were diluted in buffer that contained 100 mM KCl, flowed at $60 \mu\text{L min}^{-1}$ across probes captured at approximately 20 RU. All protein concentrations were calculated assuming homodimers were present. Data analysis to dissect thermodynamic parameters into kinetic parameters gave estimates for k_m values that ranged from 1×10^7 to $1 \times 10^9 \text{ RU M}^{-1} \text{ s}^{-1}$, values close to that predicted for a 158-kDa analyte of $3 \times 10^9 \text{ RU M}^{-1} \text{ s}^{-1}$.

homodimerisation/DNA binding, as manifested mainly by a higher rate of dissociation from DNA (data not shown).

Single truncations that did not seem to impair DNA binding (R255A, L272I, A311G and V313A) resulted in defective homodimers when combined as double or multiple mutations. DNA binding was abolished for the most heavily mutated protein, which was probably monomeric at all concentrations tested. Our results suggest that homodimerisation/DNA binding is dictated by a subset of a few key residues at the dimer interface.

Our results have strong implications for the combinatorial dimerisation of RHR family members in vivo. The selection of physiologically relevant pairings may be as much a result of kinetic factors as thermodynamic ones since rapid association and slow dissociation most likely result in nonequilibrium competitive binding.

Experimental Section

SPR instrumentation: The optical biosensor equipped with a research-grade sensor chip SA and polysorbate-20 (P20) was obtained from BIAcore AB (Uppsala, Sweden). Binding studies were

conducted on a BIAcore-3000 instrument driven by software run under Microsoft Windows 98 on a Philips Compaq DeskPro IBM-compatible PC. Data was processed with the manufacturer's BIAevaluation v.3.0 software and imported into the CLAMP software to enable global analysis.^[15]

Bacterial strains and DNA: XL1-Blue [*recA1*, *endA1*, *gyrA96*, *thi1*, *hsdR17*, *supE44*, *reclA1*, *lac(F'proAB)*, *lacI^q*, *lacZ δ M15*, *Tn10* (*tet^r*)], NM554 [*recA1*, *araD139*, Δ (*araABC-leu*)7697, Δ *lacX74*, *galU⁻*, *galK⁻*, *hsdR*, *hsdM⁺*, *rspL*, *strA*, *thi*, *mcrA*(–), *mcrB*(–)] and BW313 [HfrKL, 16 *PO/45*, [*lysA*(61–62)], *dut1*, *ung1*, *thi1*, *relA1*] strains of *Escherichia coli* were used. Bacteria were grown at 37 °C in LB broth or on agar plates, both supplemented with ampicillin (final concentration = 100 $\mu\text{g mL}^{-1}$). Oligonucleotides were either synthesized in-house on a Beckman Oligo 1000 DNA synthesizer or purchased from Gibco-BRL as customised primers.

Expression of p50RHR and p50 mutants: *E. coli* XL1-blue strain was transformed with the appropriate plasmid, plated onto LB agar that contained ampicillin (50 $\mu\text{g mL}^{-1}$) and incubated at 37 °C. Single colonies were used to inoculate LB medium (5 mL) that contained ampicillin (100 $\mu\text{g mL}^{-1}$). Cultures were grown (16 h, 37 °C, 250 rpm) and used as 1% inocula into LB medium (100 mL) with ampicillin (100 $\mu\text{g mL}^{-1}$). Cultures were incubated (37 °C, 250 rpm) until the optical density at 600 nm was 0.5. Isopropyl- β -D-thiogalactopyranoside was added (0.3 mM) and the cultures were incubated further

(2 h, 37 °C, 250 rpm). Cells were harvested by centrifugation (4000 rpm, 20 min) and lysed by sonication. Soluble lysates were analysed by SDS-PAGE, which revealed that yields of pure fusion proteins from vector pTFM4 and variants pMUT1–19 were typically around 4 mg per 100 mL culture.

Purification of p50RHR and mutants: *malE:p50RHR* genetic fusions expressed large amounts of MBP hybrid proteins, which were conveniently purified in a single-step by using affinity chromatography with amylose resin and elution with buffers (10 mM 2-[4-(2-hydroxyethyl)-1-piperazinyl]ethanesulfonic acid (Hepes), 100 mM NaCl, 3.4 mM ethylenediaminetetraacetate (EDTA) or 20 mM tris(hydroxymethyl)aminomethane (Tris)·HCl, 200 mM NaCl, 1 mM EDTA, 10 mM 2-mercaptoethanol) supplemented with maltose (10 mM). Purified proteins were judged by SDS-PAGE to be more than 90% homogenous.

Capture of biotinylated probes for SPR binding studies: Complementary pairs of single-stranded DNA fragments (both 30mers, one of the pair 5'-biotinylated) were annealed in an appropriate buffer (250 mM Tris·HCl, 500 mM NaCl, 20 mM MgCl₂) to generate the three duplex probes used in this study. The probes differed only in the sequence of the central 10 bp, which either defined a κB site or was irrelevant. Flanking sequences were random. The complementary sequences (written 5' to 3') carrying a palindromic κB site were biotin-AGTTCAGAGGGGAATTCCCAGAGACTG and GATCCAG-TACTCTCGGGAATCCCCTCTGA. The asymmetric κB site in the biotinylated strand was GGGACTTCC and the negative control sequence was ATCGATCGGA. Loosely bound streptavidin was removed from the sensor chip surface by injection of three consecutive 1-min pulses of NaCl (1 M) in NaOH (10 mM) with Milli-Q water as the running buffer. Freshly annealed biotinylated ligands were diluted in Milli-Q water and injected across individual flow cells to the desired capture levels, typically 10 RU for kinetic studies and 100 RU for near-equilibrium studies. A 1-min pulse of NaCl (1 M) in NaOH (10 mM) was applied to regenerate the surface.

Running buffers: DNA binding was explored in three different buffer systems at pH 7.4. For convenience, preliminary studies were conducted in a simple, physiologically relevant BIA-certified HBS-P buffer (10 mM Hepes, 150 mM NaCl and 0.005% P20). An alternative buffer mimicked electrophoretic mobility shift assay binding conditions reported previously^[16] (10 mM Tris·HCl, 100 mM KCl, 0.2 mM EDTA, 10% glycerol, 3 mM dithiothreitol, 0.02% Triton X-100). In that report, the binding of p50 homodimers was found to be insensitive to the nature of the monovalent cation (Na or K). A compromise was therefore made in designing the final buffer in which most binding studies were conducted (10 mM Hepes, 100 mM NaCl, 3.4 mM EDTA, 0.005% P20). All buffers were prepared fresh, filtered (0.2 μm) and degassed prior to use.

SPR with low density surfaces: Freshly purified MBP fusion proteins were diluted twofold and serially into running buffer to nanomolar concentrations (assuming dimers were present). Each protein was screened at three concentrations within the range 320–5 nM. Interaction analysis was performed at 25 °C and at a flow rate of 60 μL min⁻¹. Association and dissociation phases were typically 3 and 10 min, respectively. Depending on the buffer system employed, a single 20-s pulse of either, 1) NaCl (1 M) in NaOH (10 mM), 2) NaCl (2 M) or 3) SDS (0.07%) was applied to regenerate the sensor surface. SDS was incompatible with the potassium-containing buffer. Protein samples were randomised and injected from snap-capped single-use plastic vials. Unmodified streptavidin served as a reference flow cell.

SPR with dense surfaces: Duplex DNA fragments that contained either an asymmetric κB site or a random sequence were captured

on individual flow cells to a level of 100 RU. Freshly purified protein was injected at a flow rate of 5 μL min⁻¹ at eight different concentrations spanning the 1000–0.46 nM range (assuming dimers present), which were produced by threefold serial dilutions in running buffer. Association and dissociation phases were 8 and 1 min long, respectively. A single 1-min pulse of NaCl (1 M) in NaOH (10 mM) was applied to regenerate the sensor surface.

Data processing and analysis: Application of proper data processing methods afforded data suitable for kinetic interpretation.^[17] While this work was in progress, Michalopoulos and Hay reported a study that used gel electrophoresis and SPR to investigate the effect of mutation of key lysine residues involved in NF-κB p50 homodimer DNA binding.^[18] These authors reported that their SPR data could not be fitted to the theoretical binding models of the evaluation software and accordingly only interpreted their results qualitatively. In our work, subtraction of the bulk refractive index changes generated over an unmodified streptavidin surface referenced the data. Subtraction of the response from an average buffer injection removed systematic artefacts that occurred equally in all injections. At least three binding curves obtained from a serial dilution were analysed globally by using a mass transport model: $A_0 = A$, $A + B = AB$, where A_0 represents the injected protein concentration at time = 0, A is the concentration of the same protein near the surface, B is the immobilized probe concentration and AB that of the complex on the sensor.^[12] The forward and reverse rates of the first equilibrium ($A_0 = A$) were described by a mass transport constant (k_m) that accounted for the diffusive movement of the analyte between the compartments. Association and dissociation rate constants for complex formation were described by k_a and k_d respectively, the quotient of which gave the affinity, $K_D = k_d/k_a$.

We thank the Biotechnology and Biological Sciences Research Council for support of this work through provision of a project grant and Dr. D. J. Hart for helpful advice and discussions.

- [1] R. Sen, D. Baltimore, *Cell* **1986**, *46*, 705–716.
- [2] A. S. Baldwin, Jr., *Annu. Rev. Immunol.* **1996**, *14*, 649–681; T. D. Gilmore, *Cell* **1990**, *62*, 841–843; T. D. Gilmore, P. J. Morin, *Trends Genet.* **1993**, *9*, 427–433.
- [3] M. Grilli, J. J. Chiu, M. J. Lenardo, *Int. Rev. Cytol.* **1993**, *143*, 1–62; A. A. Beg, A. S. Baldwin, Jr., *Genes Dev.* **1993**, *7*, 2064–2070; E. B. Traenckner, H. L. Pahl, T. Henkel, K. N. Schmidt, S. Wilk, P. A. Bauerle, *EMBO J.* **1995**, *14*, 2876–2883; N. L. Malinin, M. P. Boldin, A. V. Kovalenko, *Nature* **1997**, *385*, 540–544; U. Siebenlist, G. Franzoso, K. Brown, *Annu. Rev. Cell. Biol.* **1994**, *10*, 405–455; P. A. Baeuerle, T. Henkel, *Annu. Rev. Immunol.* **1994**, *12*, 141–179.
- [4] L. Emorine, M. Keuhl, L. Weir, P. Leder, E. E. Max, *Nature* **1983**, *304*, 447–449; A. S. Baldwin, Jr., P. A. Sharp, *Proc. Natl. Acad. Sci. USA* **1988**, *85*, 723–727; K. Leung, G. J. Nabel, *Nature* **1988**, *333*, 776–778; J. Whelan, P. Ghersa, R. H. van Huijsduijnen, J. Gray, G. Chandra, F. Talabot, J. F. DeLamorter, *Nucleic Acids Res.* **1991**, *19*, 2645–2653; H. Shimizu, K. Mitomo, T. Watanabe, S. Okamoto, K.-I. Yamamoto, *Mol. Cell Biol.* **1990**, *10*, 561–568; N. L. Paul, M. J. Lenardo, K. D. Novak, T. Sarr, W.-L. Tang, N. H. Ruddle, *J. Virol.* **1990**, *64*, 5412–5419; D. Ron, A. R. Brasier, K. A. Wright, J. Tate, J. F. Hebenner, *Mol. Cell Biol.* **1990**, *10*, 4389–4395; J. L. Williams, J. Garcia, D. Harrich, L. Pearson, F. Wu, R. Gaynor, *EMBO J.* **1990**, *9*, 4435–4442; M. P. Duyao, A. G. Buckler, G. E. Sonenshein, *Proc. Natl. Acad. Sci. USA* **1990**, *87*, 4727–4731.
- [5] G. Ghosh, G. van Duyne, S. Ghosh, P. B. Sigler, *Nature* **1995**, *373*, 303–310; C. W. Muller, F. A. Rey, M. Sodeoka, G. L. Verdine, S. C. Harrison, *Nature* **1995**, *373*, 311–317; M. Sodeoka, C. J. Larson, L. Chen, W. S. Lane, G. L. Verdine, *Bioorg. Med. Chem. Lett.* **1993**, *3*, 1095–1100.

- [6] L. L. Sengchanthalangsy, S. Datta, D. Huang, E. Anderson, E. H. Braswell, G. Ghosh, *J. Mol. Biol.* **1999**, *289*, 1029–1040.
- [7] D. J. Hart, R. E. Speight, J. D. Sutherland, J. M. Blackburn, *J. Mol. Biol.* **2001**, *310*, 563–575.
- [8] R. E. Speight, D. J. Hart, J. D. Sutherland, J. M. Blackburn, *Chem. Biol.* **2001**, *8*, 951–65.
- [9] L. Galio, S. Briquet, C. Vaquero, *Biochem. Biophys. Res. Commun.* **1999**, *264*, 6–13.
- [10] D. J. Hart, R. E. Speight, M. A. Cooper, J. D. Sutherland, J. M. Blackburn, *Nucleic Acids Res.* **1999**, *27*, 1063–1069.
- [11] C. B. Phelps, L. L. Sengchanthalangsy, S. Malek, G. Ghosh, *J. Biol. Chem.* **2000**, *275*, 24392–24399.
- [12] D. G. Myszka, X. He, M. Dembo, T. A. Morton, B. Goldstein, *Biophys. J.* **1998**, *75*, 583–594.
- [13] D. B. Huang, T. Huxford, Y. Q. Chen, G. Ghosh, *Structure (Cambridge, MA, U.S.)* **1997**, *5*, 1427–1436.
- [14] C. S. Duckett, N. D. Perkins, T. F. Kowalik, R. M. Schmid, E. S. Huang, A. S. Baldwin, Jr., G. J. Nabel, *Mol. Cell. Biol.* **1993**, *13*, 1315–1322.
- [15] D. G. Myszka, T. A. Morton, *Trends Biochem. Sci.* **1998**, *23*, 149–150.
- [16] M. Kretzschmar, M. Meisterernst, C. Scheidereit, G. Li, R. G. Roeder, *Genes. Dev.* **1992**, *6*, 761–774.
- [17] D. G. Myszka, *J. Mol. Recognit.* **1999**, *12*, 279–284.
- [18] I. Michalopoulos, R. T. Hay, *Nucleic Acids Res.* **1999**, *27*, 503–509.

Received: 26 February, 2002

Revised version: 10 September, 2002 [F371]